

# Integration of Bragg grating sensors in components made of carbon fiber reinforced polymers

*Theresia Sauer<sup>1,\*</sup>, Stefan Kefer<sup>2,\*</sup>, Wolfgang Ruppert<sup>1</sup>, Ralf Hellmann<sup>2</sup> and Michael Kaloudis<sup>1</sup>*

<sup>1</sup>Laboratory for Packaging and Interconnection Technology, University of Applied Sciences  
Aschaffenburg, Wuerzburger Strasse 45, 63743 Aschaffenburg, Germany

<sup>2</sup>Applied Laser and Photonics Group, University of Applied Sciences Aschaffenburg, Wuerzburger  
Strasse 45, 63743 Aschaffenburg, Germany

\*E-mail: [Theresia.Sauer@th-ab.de](mailto:Theresia.Sauer@th-ab.de); [Stefan.Kefer@th-ab.de](mailto:Stefan.Kefer@th-ab.de)

## Abstract

This contribution discusses the integration of polymer planar Bragg grating sensors (PPBG) into carbon fiber reinforced polymer (CFRP) components. For the first time, it is shown that PPBGs based on cyclic olefin copolymers can be integrated into commercial-grade composites, thereby withstanding the demanding production processes. Pre-impregnated fibers are stacked and partially modified to form a sensor pocket. Afterwards, the CFRP specimen containing the optical sensor is cured in a heated mechanical press for 2 hours at a pressure of 7 bar and a temperature of 120 °C. A subsequent evaluation of the sensor signal shows a Bragg wavelength shift of 1236 pm and a decline in signal amplitude of -2 dB. Three-point flexural tests of the cured sample reveal a linear behavior of the sensor signal towards external loads. The determined sensitivity in dependence of the CFRP specimen's maximum central deflection is -112 pm/mm, while correlation to the applied force results in a sensitivity of -5 pm/N.

**Keywords:** Bragg grating sensors, carbon fiber reinforced polymers, cyclic olefin copolymers, structural health monitoring

## Introduction

Due to their outstanding mechanical properties - excellent strength combined with low weight and density - the usage of carbon fiber reinforced polymers (CFRP) for lightweight and high-performance applications, such as the aerospace industry, has increased dramatically over the last few years. However, in comparison to classical materials, composites tend to behave inherently different in excess load situations. In the case of metals, applied forces will cause elastic deformations which will then turn to plastic distortions when crossing the material's yield point. A further load increase will ultimately lead to cracks, fractures and the apparent breakdown of a metal workpiece. Predicting the failure process of CFRPs on the other hand is a challenging and elaborate task since even microscopically small fissures, especially at critical points, can cause sudden and unpredictable failure of a CFRP component [1]. Therefore, immense effort has to be invested in the detection of damage and material fatigue. While there are several approaches for live structural health monitoring of composites, most damage inspection methods are based on offline testing

procedures. Thus, in order to reduce costs for manufacturers while simultaneously mitigating user safety concerns, alternative technologies enabling detection of structural changes in CFRPs need to be developed.

In recent years, the integration of silica-based fiber Bragg grating (FBG) sensors has proven to be a promising method for in-situ evaluation of composite materials. Albeit, their inherent one-dimensionality needs to be addressed by employing complex sensor structures, e.g. a multicore FBG, in order to enable quantification of multidimensional forces [2,3]. Polymer planar Bragg gratings (PPBG) however, offer up to three-dimensional detection of deformations [4,5]. Additionally, polymer-based optical Bragg grating sensors exhibit increased sensitivity towards stress and strain due to their distinctly low Young's modulus. However, the insufficient glass transition temperature of most PPBG-substrates prevents successful integration into commercial CFRPs, since these polymers cannot withstand harsh fabrication processes.

This challenge can be overcome by employing PPBGs based on cyclic olefin copolymers (COC). Due to outstanding glass transition temperatures of up to 250 °C, this substrate

material is able to outlast temperature measurements up to 160 °C [6,7]. Additionally, COC-PPBGs are inherently unsusceptible towards relative humidity fluctuations [8,9]. Thus, they represent a particularly auspicious sensor concept for CFRP integration.

## Fundamentals

In principal, PPBGs are constituted of a polymer substrate featuring a waveguide and a Bragg grating, as depicted in Fig. 1.

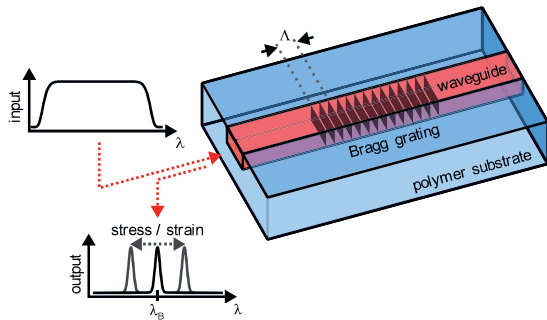


Fig. 1: Schematic of a polymer planar Bragg grating sensor.

Thereby, the Bragg grating is a periodic refractive index modulation which acts as a narrowband reflector for light traversing the waveguide. Its main reflection wavelength, denoted as Bragg wavelength  $\lambda_B$ , is defined by the effective refractive index  $n_{\text{eff}}$  and the grating period  $\Lambda$  according to Eq. (1).

$$\lambda_B = 2n_{\text{eff}}\Lambda$$

External forces will affect  $\Lambda$  and  $n_{\text{eff}}$  resulting in a proportional shift of  $\lambda_B$ , which can be detected and evaluated.

Waveguide and Bragg grating are generated simultaneously within the COC (TOPAS6017S-04, TOPAS Advanced Polymers) by irradiating the substrate with ultraviolet radiation generated by a KrF excimer laser (BraggStar Industrial, Coherent). A sophisticated discussion of the employed manufacturing method, denoted as single-writing-step procedure, is given by the authors and others elsewhere [10–12]. Fig. 2 shows the fabricated COC-PPBG before its integration into a CFRP-specimen. In order to couple the PPBG to the evaluation unit, a physical connection with a single-mode fiber (SMF) needs to be established. This is achieved by butt-coupling an optical fiber to the waveguide by means of a UV-curable adhesive (NOA 61, Norland). Evaluation of the reflected sensor signal is done by an industrial-grade interrogation unit (HYPERION si155, MICRONOPTICS).

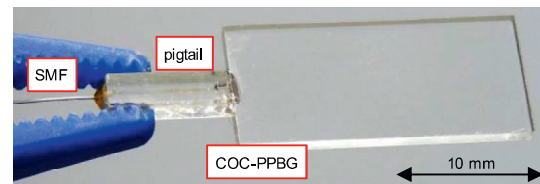


Fig. 2: COC-PPBG butt-coupled to a pigtailed standard single-mode fiber.

Carbon fiber reinforced polymers are a composite material consisting of at least two components, carbon fibers embedded in a polymer matrix (mostly epoxy resin). While the matrix serves as parent material, the fibers are responsible for absorption and redistribution of external forces, which yields components exhibiting outstanding strength-to-weight ratios. The final mechanical properties of CFRPs are thereby highly dependent on the used materials. Additionally, amount and direction of the fibers enclosed within the workpiece plays an important role. This leads to distinct anisotropic behavior of single-layer CFRP components, which is mitigated by stacking layers with alternating fiber orientations on top of each other. For commercial manufacturing of CFRPs, it is common to make use of pre-impregnated composite fibers known as prepreps, a compound of semi-cured epoxy with embedded fiber structures. Multiple prepreg layers are preformed into desired shapes and afterwards fully cured at high temperatures, and under immense pressure, thus chemically crosslinking the matrix system to generate operational CFRP components.

## Sample preparation and sensor integration

Nine prepreg layers (P3252S-25, TORAYCA) with a fiber orientation of  $\pm 45^\circ$  are cut to rectangular shape and stacked on top of each other to form a CFRP specimen. While the outer two layers remain unaltered, the middle section needs to be modified in order to form a sensor pocket. This prevents uneven pressure distributions during the curing procedure and guarantees a flat surface of the specimen. Fig. 3 elucidates the preparation process. After inserting the sensor into its predefined location, the prepreg stack is positioned on a brass foil to prevent the CFRP matrix from sticking to the curing apparatus.

Most commercial manufacturers of CFRP components use autoclaves for the final curing procedure. For simple planar specimens however, it is possible to use a heated press in order to generate workpieces with comparable properties.

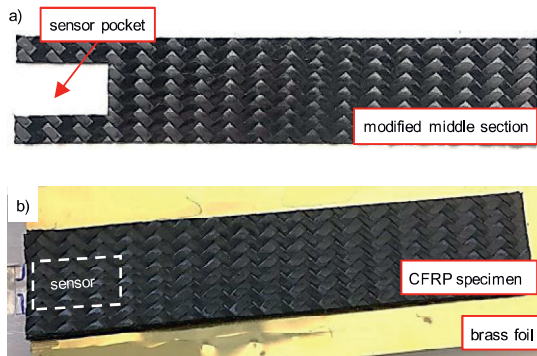


Fig. 3: a) Modified middle-section prepreg and b) CFRP sample with embedded PPBG sensor before curing.

The heated press used for curing the CFRP workpiece, equipped with a PPBG, is depicted in Fig. 4.

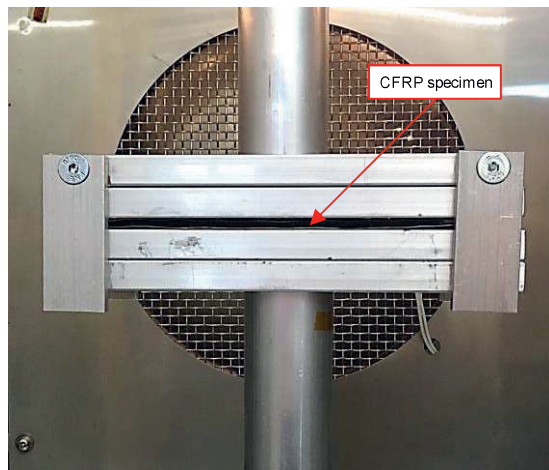


Fig. 4: Curing setup - mechanical press inside air circulated furnace.

The CFRP prepreg stack is placed in-between the plates of the press which are positioned inside an air circulated furnace. Both plates are actively controlled by a tensile test machine (Autograph AG-X 20kN, SHIMADZU). This way, constant pressure is applied to the specimen throughout the whole curing process. An overview on the applied curing parameters is given in Tab. 1.

Tab. 1: Curing parameters

Pressure	7 bar
Temperature	120 °C
Duration	2 h

Removing the specimen from the press after curing reveals that some of the epoxy has leaked from the prepreg stack. An image of the cured sample can be seen in Fig. 5 a), while

Fig. 5 b) shows the PPBG signal before and after curing of the sample.

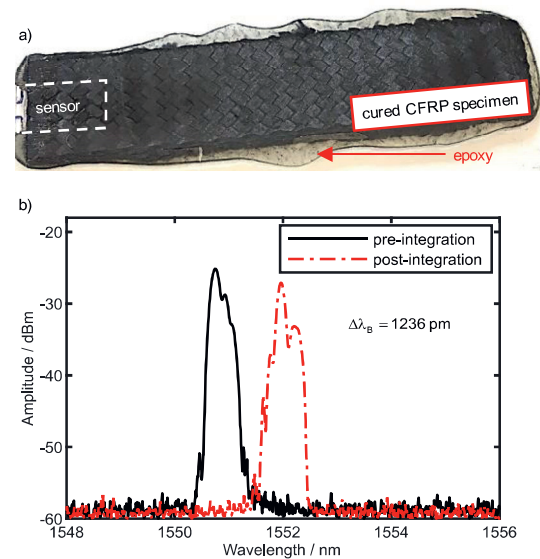


Fig. 5: a) CFRP specimen after curing and b) PPBG sensor signal pre and post curing.

Even after being exposed to the harsh curing process parameters, the sensor delivers a strong and evaluable signal. The findings demonstrate that COC-PPBGs are suitable for integration into commercial composite structures. However, the cured CFRP introduces constant force on the embedded sensor, which results in a positive Bragg wavelength shift of 1236 pm and a peak amplitude reduction of -2 dB.

In order to assess the connection of the CFRP prepregs with the integrated sensor, the specimen was examined via computed tomography (CT) scans. After finishing all experiments on the specimen, microsections were used to verify the CT scan. The results of both investigation methods are summarized in Fig. 6.



Fig. 6: a) CT scan and b) microsection of CFRP-integrated PPBG.

Both images reveal air pockets in close vicinity to the integrated sensor. Their existence can be correlated to the modification of the prepreg layers prior to embedding the sensor, which introduces air-filled voids within the specimen.



Although while cured, the epoxy becomes viscous, it is not able to completely refill these voids. This circumstance can be mitigated by adjusting the geometry of the PPBG substrate so the need for prepreg modification is reduced or even omitted completely.

### Experimental results

After removing the excess epoxy on the outer edges of the test sample, examination of the integrated PPBG's sensing capabilities is done by using a three-point flexural test configuration, as shown in Fig. 7.

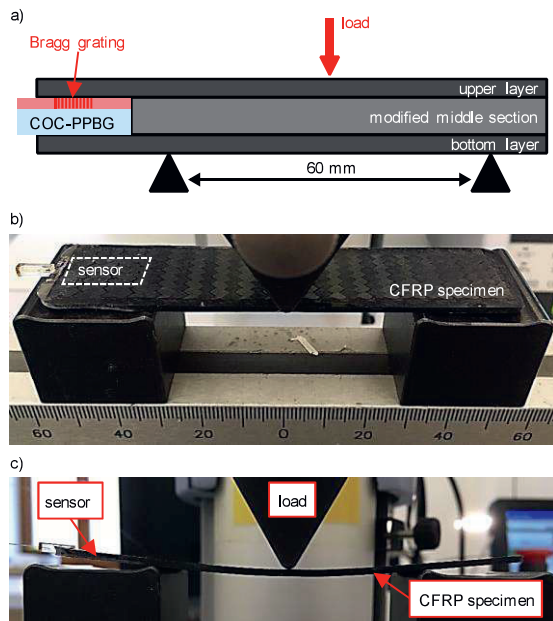


Fig. 7: a) Schematic and b) image of the employed three-point flexural test setup. Section c) shows the bent CFRP specimen at a maximum stroke of 2 mm.

Thereby, the sensor inside the specimen has no contact with the support spans and its minimum distance from the loading point is 40 mm. This configuration enables a defined bending of the specimen while it ensures that the PPBG detects deformation by flexural forces only. The maximum deflection at the center of the sample, denoted as stroke, is actively controlled by a tensile test machine (EZ-L, SHIMADZU). The system also determines the force which is necessary to reach a predefined stroke value. Fig. 8 depicts the temporal evolution of a three-point flexural test cycle. Prior to the experiment, the tensile testing machine applies a pre-load of 3 N to the specimen. Therefore, the stroke curve starts with an offset of 0.35 mm. Afterwards, the stroke is increase with a speed of 8 mm/min until it reaches its maximum at 2 mm.

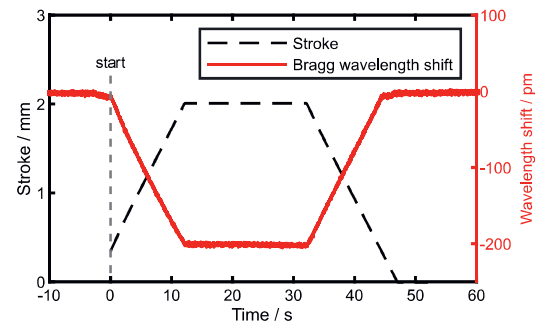


Fig. 8: Temporal evolution of the Bragg wavelength during a three-point flexural test with a maximum stroke of 2 mm.

This value is held constant for 20 s before reducing the load at similar speed until the specimen relaxes completely. Fig. 8 indicates that applying external loads to the workpiece leads to a negative shift of the sensor's Bragg wavelength. Thereby, the absolute wavelength shift can be correlated directly to the specimen's degree of bending. Since the actual sensitive element, the Bragg grating structure, is located close to the surface of the CFRP sample (c.f. Fig. 7), the bending process leads to a reduction of its grating period which in turn results in a shift of the Bragg signal towards shorter wavelengths. The maximum wavelength shift is -205 pm at a stroke of 2 mm. At the end of a cycle, it returns to its original value after removing the load from the sample.

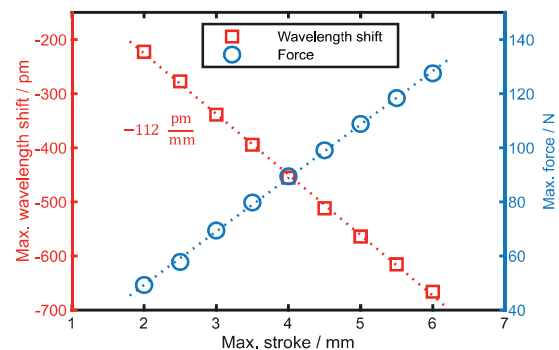


Fig. 9: Maximum wavelength shift and applied force as a function of maximum stroke during a three-point flexural testing cycle.

With increasing maximum stroke, the maximum Bragg wavelength shift follows in a linear fashion, as depicted in Fig. 9. In this configuration and within the examined range, the PPBG exhibits a sensitivity of -112 pm/mm. Thus, depending on the used interrogation device, which offer wavelength resolutions down to 1 pm, it enables detection of minor

displacements of the CFRP specimen [13]. By simultaneously tracking the force which is necessary to deflect the sample to maximum stroke, it is possible to correlate the wavelength shift to the applied load, resulting in a sensitivity of -5 pm/N.

## Conclusion

In summary, it was shown that COC-based PPBGs are able to outlast the demanding production parameters of a commercial CFRP component, where the optical sensor is exposed to pressures up to 7 bar and temperatures up to 120 °C for at least 2 hours. To the best of the authors' knowledge, this is the first polymer-based optical sensor which is capable of withstanding an integration process this harsh without exhibiting noticeable losses in signal quality. Three-point flexural tests reveal a linear correlation of the sensor's Bragg wavelength shift with the applied loads. In the examined regime, up to a maximum stroke of 6 mm, the PPBG's sensitivity was determined as -112 pm/mm, or -5 pm/N, respectively. Metallographic investigations of the CFRP specimen show air pockets in close vicinity to the integrated sensor which underlines the demand for optimized sensor substrate designs for future investigations. Based on these results, COC-PPBGs constitute a promising concept for the integration into commercial CFRP products, enabling in-situ structural health monitoring of composites with outstanding sensitivity.

## Acknowledgements

This work has been funded by the VDI/VDE-IT on behalf of the Bavarian Ministry of Economic Affairs, Regional Development and Energy.

## References

- [1] A. Zaman, S. A. Gutub, and M. A. Wafa, *Journal of Reinforced Plastics and Composites* 32, 24, 1966–1988 (2013); doi: 10.1177/0731684413492868.
- [2] G. Zhou, and L. M. Sim, *Smart Materials and Structures* 11, 6, 925–939 (2002); doi: 10.1088/0964-1726/11/6/314.
- [3] F. Khan, A. Denasi, D. Barrera, J. Madrigal, S. Sales, and S. Misra, *IEEE Sensors Journal*, 1 (2019); doi: 10.1109/jsen.2019.2905010.
- [4] M. Rosenberger, W. Eisenbeil, B. Schmauss, and R. Hellmann, *Sensors* 15, 2, 4264–4272 (2015); doi: 10.3390/s150204264.
- [5] M. Rosenberger, H. Pauer, M. Girschikofsky, H. Woern, B. Schmauss, and R. Hellmann, *IEEE Photonics Technology Letters* 28, 17, 1898–1901 (2016); doi: 10.1109/LPT.2016.2574889.
- [6] G. Khanarian, *Optical Engineering* 40, 6, 1024 (2001); doi: 10.1117/1.1369411.
- [7] M. Rosenberger, S. Kefer, M. Girschikofsky, G.-L. Roth, S. Hessler, S. Belle, B. Schmauss, and R. Hellmann, *Optics Letters* 43, 14, 3321–3324 (2018); doi: 10.1364/OL.43.003321.
- [8] W. Yuan, L. Khan, D. J. Webb, K. Kalli, H. K. Rasmussen, A. Stefani, and O. Bang, *Optics Express* 19, 20, 19731–19739 (2011); doi: 10.1364/OE.19.019731.
- [9] M. Rosenberger, S. Hessler, S. Belle, B. Schmauss, and R. Hellmann, *Sensors and Actuators A: Physical* 221, 148–153 (2015); doi: 10.1016/j.sna.2014.10.040.
- [10] M. Rosenberger, G. Koller, S. Belle, B. Schmauss, and R. Hellmann, *Optics Express* 20, 25, 27288–27296 (2012); doi: 10.1364/OE.20.027288.
- [11] M. Rosenberger, B. Schmauss, and R. Hellmann, *Optical Materials Express* 6, 6, 2118 (2016); doi: 10.1364/OME.6.002118.
- [12] S. Hessler, M. Rosenberger, B. Schmauss, and R. Hellmann, *Optical Materials* 75, 230–235 (2018); doi: 10.1016/j.optmat.2017.10.029.
- [13] D. Tosi, *Sensors* 17, 10, 2368 (2017); doi: 10.3390/s17102368.